ARMC4 Mutations Cause Primary Ciliary Dyskinesia with Randomization of Left/Right Body Asymmetry

Rim Hjeij,[1] Anna Lindstrand,[2] Richard Francis,[3] Maimoona A. Zariwala,[4] Xiaoqin Liu,[3] You Li,[3] Rama Damerla,[3] Gerard W. Dougherty,[1] Marouan Abouhamed,[1] Heike Olbrich,[1] Niki T. Loges,[1] Petra Pennekamp,[1] Erica E. Davis,[2] Claudia M.B. Carvalho,[5] Davut Pehlivan,[5] Claudius Werner,[1] Johanna Raidt,[1] Gabriele Köhler,[1] Karsten Häffner,[6] Miguel Reyes-Mugica,[7] James R. Lupski,[5] Margaret W. Leigh,[8] Margaret Rosenfeld,[9] Lucy C. Morgan,[10] Michael R. Knowles,[11] Cecilia W. Lo,[3] Nicholas Katsanis,[2] and Heymut Omran[1,*]

The motive forces for ciliary movement are generated by large multiprotein complexes referred to as outer dynein arms (ODAs), which are preassembled in the cytoplasm prior to transport to the ciliary axonemal compartment. In humans, defects in structural components, docking complexes, or cytoplasmic assembly factors can cause primary ciliary dyskinesia (PCD), a disorder characterized by chronic airway disease and defects in laterality. By using combined high resolution copy-number variant and mutation analysis, we identified *ARMC4* mutations in twelve PCD individuals whose cells showed reduced numbers of ODAs and severely impaired ciliary beating. Transient suppression in zebrafish and analysis of an ENU mouse mutant confirmed in both model organisms that ARMC4 is critical for left-right patterning. We demonstrate that ARMC4 is an axonemal protein that is necessary for proper targeting and anchoring of ODAs.

Cilia are highly organized and evolutionarily conserved microtubule-based organelles likely composed of several hundred proteins.[1] In contrast to primary cilia, which are likely chemosensory and are present in almost all cell types, motile cilia generate active beating through dynein motors and associated complexes in only certain cell types, such as respiratory epithelium.[2] In humans, mutations in genes that comprise structural components or factors that regulate assembly of these structural components result in primary ciliary dyskinesia (PCD, MIM 244400).[3] To date, mutations in 19 genes have been reported to cause PCD; however, no mutations have ever described a functional role for targeting these complexes.

We used copy-number variation (CNV) analysis to accelerate discovery of PCD-causing mutations. In contrast to point mutations, the contribution of CNVs in ciliary disorders is poorly defined, and large deletions have been reported in disorders of motile cilia only on rare occasions.[4] To overcome this challenge, we generated a custom high-resolution oligonucleotide array-CGH containing probes for 772 genes prioritized from the ciliary proteome (see Table S1 available online), which we used to screen a cohort of 96 ciliopathy individuals. Signed and informed consent was obtained from all participants and family members according to protocols approved by the Institutional Ethics Review Boards at the University of Muenster and Freiburg as well as collaborating institutions.

We identified a homozygous deletion in individual OP-589II1 (chr10: 28270060–28275320), which encompassed exons 4–7 of *ARMC4* (NM_018076.2, Figures S1A and S1B). This genomic variant was not present in either 229 healthy controls or in the Database of Genomic Variants. This CNV segregated with the disease status in the PCD family OP-589 because the other affected sibling OP-589II2 also carried the same homozygous deletion. Cross-breakpoint PCR amplification (Figure S1C) showed that the deletion encompassed 8.406 kb that span exons 4 through 7 of *ARMC4* and is predicted to induce a premature termination, consistent with a loss-of-function mutation.

We targeted our sequencing analyses to 135 PCD individuals with ODA defects documented by transmission electron microscopy (TEM) and/or immunofluorescence (IF) analysis. We found a homozygous variant c.2780T>G predicting a p.Leu927Trp missense mutation in an evolutionarily conserved region (Figure 1; Figure S2). This variant is not present in the 1000 Genomes Database (and PolyPhen-2 predicts altered function with a damage score of 1.00). Additionally, we found *ARMC4* homozygous and compound heterozygous mutations in eight additional PCD families, all predicting premature termination of translation. In total, we identified *ARMC4* mutations in 12 PCD individuals from 10 families that segregated with the disease status in an autosomal-recessive inheritance

[1]Department of General Pediatrics, University Children's Hospital Muenster, 48149 Muenster, Germany; [2]Center for Human Disease Modeling, Duke University Medical Center, Durham, NC 27710, USA; [3]Department of Developmental Biology, University of Pittsburgh School of Medicine, Pittsburgh, PA 15201, USA; [4]Department of Pathology and Laboratory Medicine, UNC School of Medicine, University of North Carolina, Chapel Hill, NC 27599, USA; [5]Department of Molecular and Human Genetics, Baylor College of Medicine, Houston, TX 77030, USA; [6]University Hospital Freiburg, 79106 Freiburg, Germany; [7]Department of Pathology, University of Pittsburgh School of Medicine, Pittsburgh, PA 15232, USA; [8]Department of Pediatrics, UNC School of Medicine, Chapel Hill, NC 27599, USA; [9]Seattle Children's Hospital and University of Washington School of Medicine, Seattle, WA 98105, USA; [10]Department of Respiratory Medicine, Concord Hospital, Concord 2139, Australia; [11]Department of Medicine, UNC School of Medicine, Chapel Hill, NC 27599, USA
*Correspondence: heymut.omran@ukmuenster.de
http://dx.doi.org/10.1016/j.ajhg.2013.06.009.

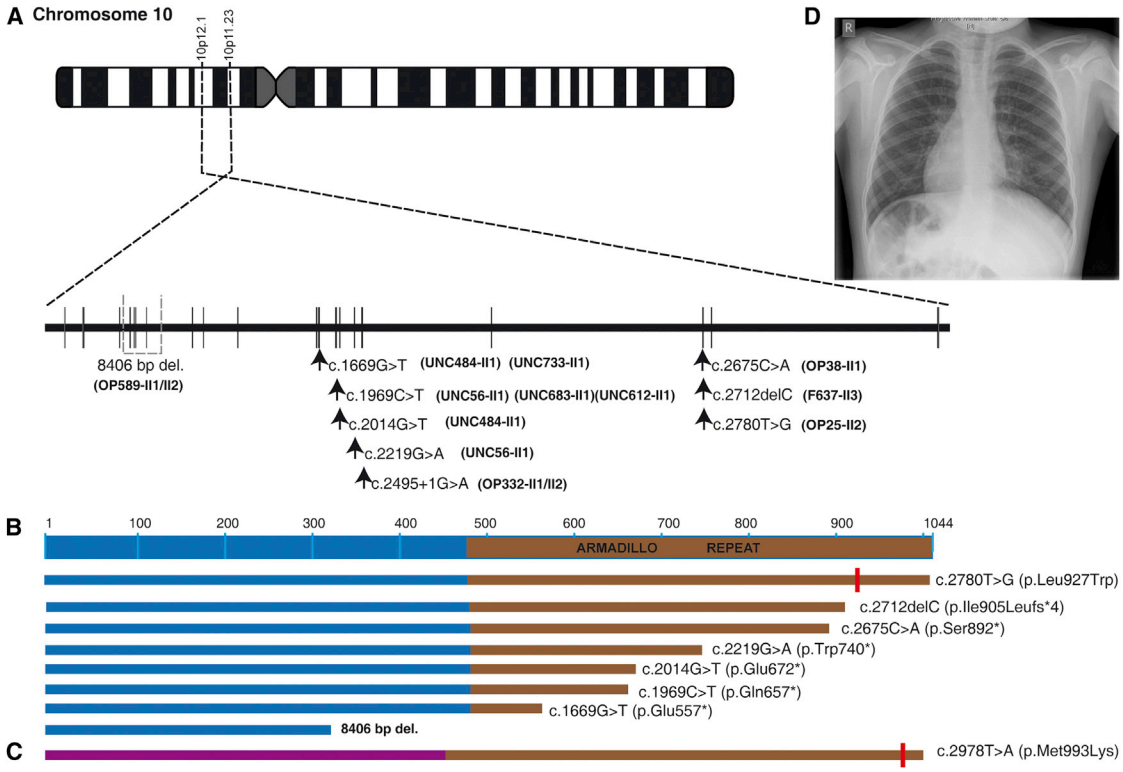

Figure 1. *ARMC4* Mutations in Human PCD Individuals and in Mice
(A) Schematic of chromosome 10 and genomic structure of *ARMC4*. The positions of the identified mutations are indicated by black arrows, the position of the 8.4 kb deletion is indicated by dashed lines.
(B) Schematic of the relative positions of *ARMC4* mutations identified in PCD individuals in the ARMC4 coding sequence. One mutation is a deletion, six lead to a premature stop and one is a missense mutation exchanging leucine with tryptophan at the position 927 (vertical red bar).
(C) *Aotea Armc4* mutant mouse carrying the missense mutation (vertical red bar) represents methionine exchanged with lysine at the position 993 (equivalent to human Met1000).
(D) Chest X-ray of individual OP-38II1 shows situs inversus totalis (dextrocardia, gastric bubble right, liver on the left) and left paracardial opacities with cystic lesions suggestive for middle lobe atelectasis and bronchiectasis.

pattern (Table S2). All affected individuals displayed a clinical phenotype consistent with PCD including recurrent upper and lower airway disease as well as bronchiectasis. Seven of 12 individuals had neonatal respiratory distress syndrome. Additionally, eight of the 12 affected individuals displayed situs inversus totalis and four had situs solitus. All of the tested individuals had low levels of nasal nitric oxide.[5] Thus, *ARMC4* deficiency causes PCD and randomization of left/right body asymmetry (Figure 1D; Table S2).

ARMC4, located on chromosome 10p12.1-p11.23, contains 20 exons encoding a protein of 1,044 amino acids. Although a role for *ARMC4* in ciliary function has not been reported, ARMC4 has been identified in the cilia proteome,[6] specifically in mass spectrometry studies of human bronchial epithelium and trypanosome flagella.[7,8] Its expression profile has been inferred to predict a ciliary gene,[9] and it is expressed in multiciliated airway cells.[10] Overall these data suggest an evolutionarily conserved functional role for ciliary and flagellar motility. ARMC4 has 10 Armadillo repeat motifs (ARMs) and one HEAT repeat. ARM proteins are known to be involved in a variety of processes including cell migration and proliferation, signal transduction, and maintenance of overall cell structure. It is also reported that tandem ARM-repeat units fold together as a superhelix, forming a versatile platform for interactions with many protein partners.[11]

To test whether *ARMC4* has an evolutionarily conserved role in establishing left-right asymmetry in vertebrates, we performed morpholino (MO)-based suppression of *armc4* in zebrafish (*D. rerio*) embryos. Reciprocal BLAST identified a single zebrafish *armc4* ortholog (Armc4; 58% protein sequence identity with human ARMC4). We injected two different splice-blocking MOs into embryos at the one to four cell stage, and embryo batches were scored subsequently for left-right asymmetry defects at 36 hr post-fertilization. For each MO, we independently observed a dose-dependent effect on heart looping, which resulted in randomization (rightward or absent looping; Figure 2A) at the highest doses tested due to aberrant *armc4* mRNA splicing as determined by RT-PCR (Figure S3). Coinjection of wild-type (WT) human *ARMC4* mRNA with MO resulted in significant rescue of abnormal unlooped or rightward looping phenotypes (56% versus 25% abnormal for WT

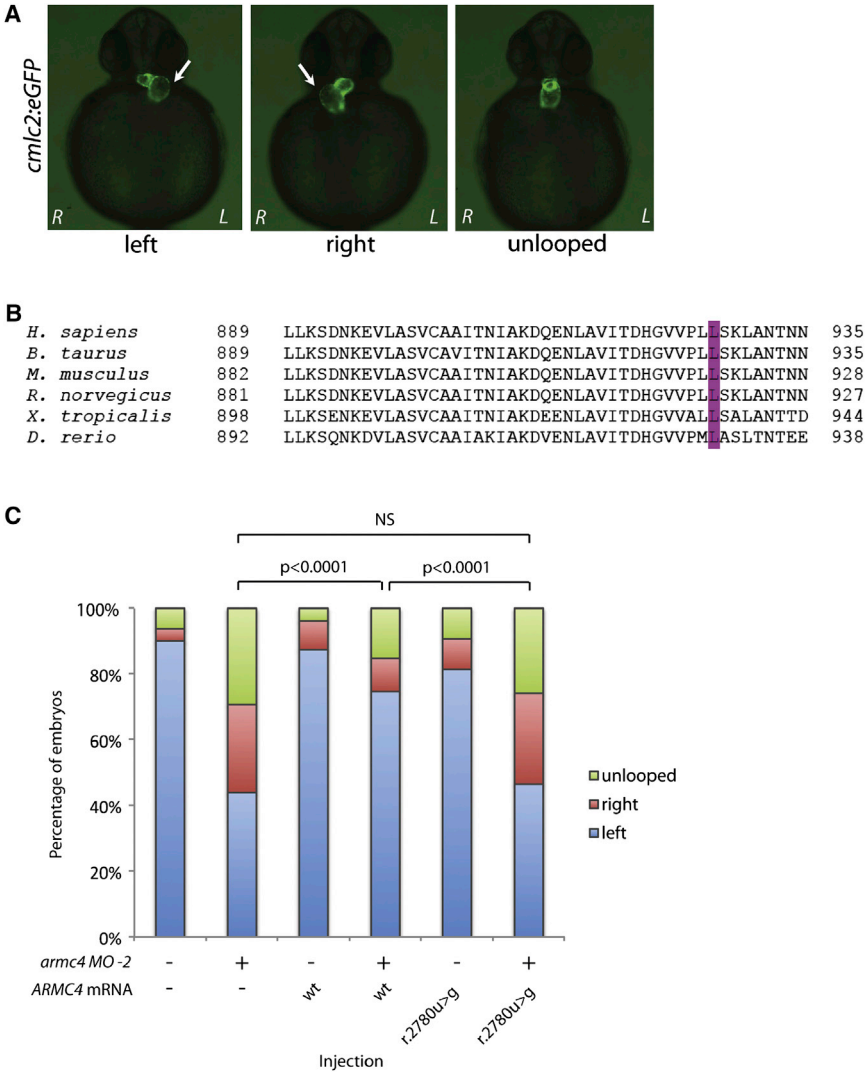

Figure 2. Rescue Experiments with Human WT *ARMC4* mRNA and In Vivo Complementation Studies of *ARMC4* r.2780u > g

(A) MO-induced suppression of *armc4* in zebrafish embryos gives rise to left-right asymmetry defects. Live embryo ventral images of *cmlc2:eGFP* morphants are shown (fluorescence overlaid with bright field). Arrows indicate heart looping direction relative to the left (L) and right (R) side of each embryo.

(B) Clustal alignment showing that leucine at position 927 is evolutionary conserved in several organisms.

(C) Quantification of live scoring of *armc4* MO and human mRNA (co)injections. *cmlc2:eGFP* embryos were injected with the indicated dose (9 ng MO-2 and/or 100 pg *ARMC4* mRNA) and scored live according to criteria shown in (A). n = 54–116 embryos per injection, repeated at least twice; with masked scoring; NS, not significant; all comparisons were made with χ^2 tests. To generate human WT and r.2780u > g encoding mRNA, we first cloned the full *ARMC4* open reading frame into the pCS2+ plasmid, linearized with NotI, and performed in vitro transcription with the SP6 mMessage mMachine kit (Ambion).

versus MO; $p < 0.0001$; n = 79–116 embryos per injection; MO-2 is shown, Figure 2C). These results confirmed a functional role for *armc4* in the establishment of left-right asymmetry.

Next, to test the pathogenicity of the homozygous c.2780T>G variant identified in the mutational screening (Figure 2B), we compared the ability of equivalent doses of *ARMC4* WT or r.2780u > g mRNA to rescue the MO-2 induced heart looping (Figure 2C). Coinjection with MO and *ARMC4* message harboring r.2780u > g resulted in aberrant heart looping phenotypes statistically indistinguishable from that of MO alone (n = 54–116 embryos per injection, scored masked for injection cocktail), demonstrating that this variant alters protein function.

We established a forward genetic screen with N-ethyl-N-nitrosurea (ENU) to examine defects of motile ciliary function in the respiratory epithelium and left-right patterning.[12] All animal studies were conducted under an Animal Study Protocol approved by the University of Pittsburgh Animal Care and Use Committee. For mouse whole-exome sequencing analysis, exon-capture was performed with the Agilent SureSelect Mouse All Exon V1 kit followed by pair-end sequencing with the SOLiD 5500xl sequencer. Reads were mapped to the B6 reference genome (mm9) with LifeScope analysis tools. Average 45× coverage was obtained, and variants were annotated with annovar and filtered with custom scripts. We identified a recessive missense mutation in *Armc4* (NM_001081393.1) in the *Aotea* mouse line (c.T2978A/p.Met993Lys; Figure 1C). This mutation segregated consistently in homozygosity among all *Aotea* mutants. Among homozygous mutants with abnormal laterality, half had situs inversus (complete reversal of heart and stomach situs, n = 14) and half exhibited heterotaxy (discordant heart and stomach situs, n = 13), indicating randomization of laterality (Figure 3A; Movie S1). We performed whole-mount in situ hybridization on mouse embryos at embryonic day E7.5 and identified specific expression of *Armc4* in the ventral node, consistent with a role in left-right axis development (Figure 3B). Analysis by histopathology showed *Aotea* mutants can have a range of cardiovascular anomalies, including right aortic arch, perimembranous and muscular ventricular septal defects, ventricular noncompaction, and anomalous venous return (Figure 3C).

Respiratory cilia of *Aotea* mutants were either immotile or had slow dyskinetic motion compared to WT animals (Movie S2). TEM analysis of tracheal airway cilia revealed

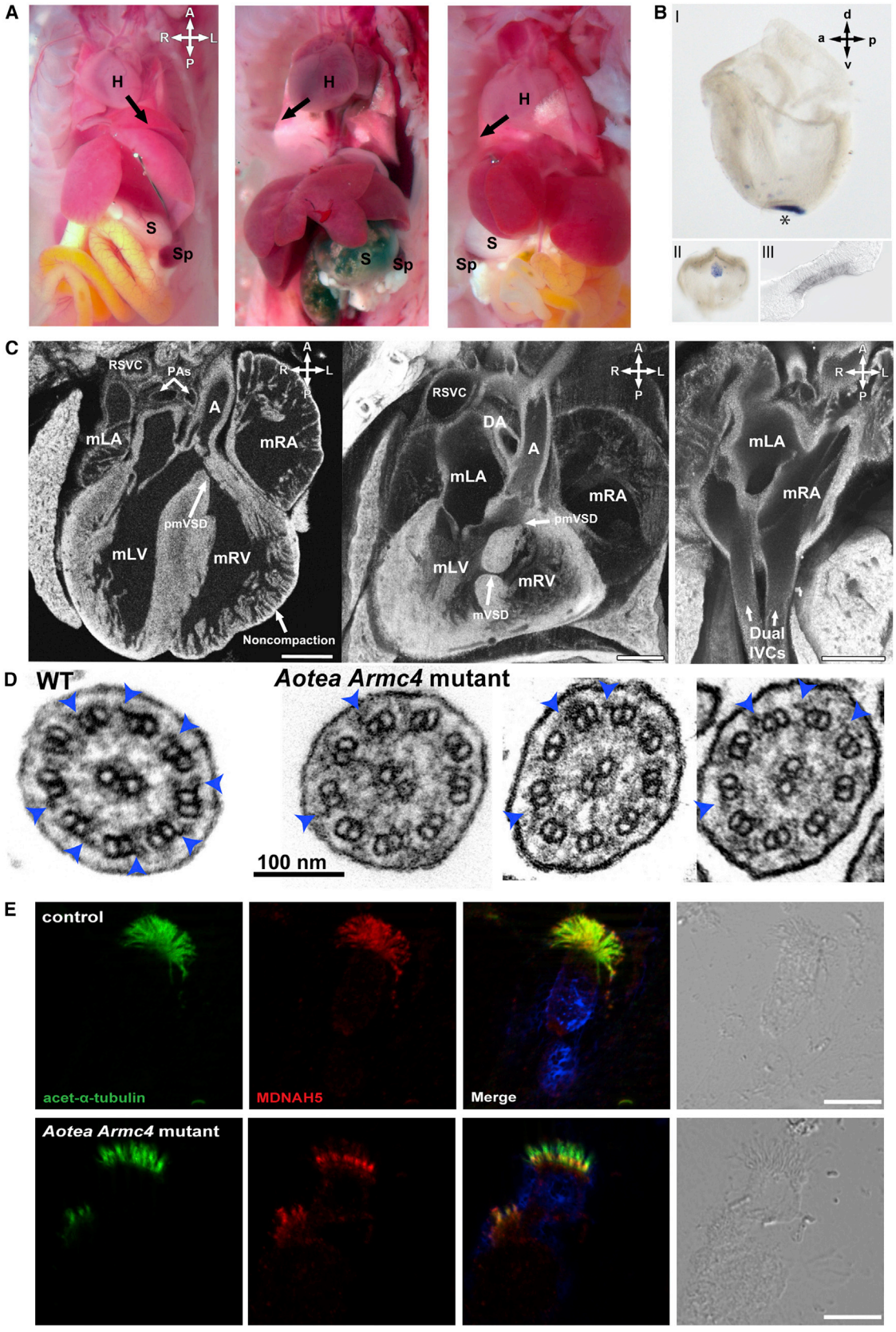

Figure 3. ***Armc4*** **Mutant Mice** ***Aotea*** **Display Organ Laterality Defects, Cardiac Anomalies, and Cilia Ultrastructural Defects**
(A) *Aotea* mutant pups can exhibit situs solitus (left), heterotaxy (middle), and situs inversus totalis (right). Arrow denotes cardiac situs with direction of heart apex orientation. Abbreviations are as follows: R, right; L, left; P, posterior; A, anterior; H, heart; S, Stomach; Sp, Spleen.

(legend continued on next page)

a marked reduction in ODAs (Figure 3D). High resolution IF microscopy of *Aotea* tracheal epithelia with antibodies to mouse axonemal dynein heavy chain MDNAH5 showed only proximal staining of MDNAH5, consistent with a defect of ODA assembly in the distal ciliary axonemes (Figure 3E). Analyses of ependymal cilia in brain slices from the *Aotea* mutants revealed that although fluid flow was generated, it was slower than in WT animals (Movie S3). Notably, *Aotea* mutants did not develop hydrocephalus during the first week of postnatal life, which is associated commonly with other mutant mouse models of PCD, such as *Mdnah5*$^{-/-}$ mice.[13] However, they develop hydrocephalus at 3 to 4 weeks of age and succumb prior to reaching reproductive age. Overall, these findings show that this recessive *Armc4* mutation in mice causes phenotypes consistent with PCD.

To understand further the functional role of ARMC4 in ODA assembly, we analyzed its subcellular localization in human motile respiratory cilia by using rabbit polyclonal anti-ARMC4 antibodies. IF microscopy identified ARMC4 localization both within the ciliary axonemes and at the ciliary base in control cells (Figure 4A). In respiratory cells from individuals with *ARMC4* mutations that predict premature termination of translation, ARMC4 localization was absent from the ciliary axonemes but remained detectable at the ciliary base (Figures 4B–4E). The latter probably represent nonspecific cross-reactivity to basal body proteins that is observed occasionally with rabbit polyclonal antibodies.[14] We conclude that ARMC4 is an axonemal component that is absent from the axonemes in all individuals with loss-of-function mutations. We next examined respiratory epithelial cells of individuals with the *ARMC4* c.2780T>G variation (Figure 4F). Here, the axonemal ARMC4 localization was not altered, indicating that the mutant ARMC4 still accumulated and localized correctly.

To explore the functional consequences of ARMC4 dysfunction, we analyzed with the SAVA system the respiratory ciliary beating in individuals with *ARMC4* mutations by high-speed videomicroscopy. Most cilia exhibited either a markedly reduced ciliary beat frequency and amplitude or complete immotility, consistent with severe ODA defects (Movies S4, S5, and S6). Notably, some c.2780T>G mutant cilia showed motility, suggesting that more ODAs can be assembled compared to cilia of individuals harboring *ARMC4* loss-of-function mutations (Movies S7 and S8). This indicates that the predicted p.Leu927Trp protein present in OP-25II2 probably retains some functionality.

Most reported PCD types are characterized by structural defects of respiratory cilia that involve outer (ODA) and/or inner (IDA) dynein arm components and/or function. Genetic studies in PCD individuals to date have identified autosomal recessive mutations in genes encoding axonemal structural subunits of the ODA complexes or related docking components such as *DNAH5* (MIM 603335), *DNAI1* (MIM 604366), *DNAI2* (MIM 605483), *DNAL1* (MIM 610062), *NME8* (formally referred to as *TXNDC3*) (MIM 607421), *DNAH11* (MIM 603339), *CCDC103* (MIM 614677), and *CCDC114* (MIM615038).[15–22] In addition, mutations in *DNAAF2* (*KTU*) (MIM 612517), *DNAAF1* (*LRRC50*) (MIM 613190), *DNAAF3* (MIM 614566), *HEATR2* (MIM 614864), and *LRRC6* (MIM 614930) encode proteins that function in cytoplasmic preassembly of axonemal dynein arm complexes and are therefore referred to as dynein axonemal assembly factors (DNAAFs).[4,23–26] Ultrastructural analysis by TEM of respiratory ciliary axonemes from individuals with *ARMC4* mutations confirmed marked reduction of ODAs (Figure 5G), indicating that ARMC4 deficiency or dysfunction causes a reduction but not a complete loss of axonemal ODA assembly. These findings are consistent with the TEM findings observed in the *Aotea Armc4* mutant mouse. Careful analyses revealed ODA abnormalities in all analyzed cross-sections, indicating that *Armc4* mutations affect ODA composure along the entire axonemal length. Interestingly, in c.2780T>G mutant cilia, more ODAs than in respiratory cilia harboring loss-of-function mutations were assembled consistent with a partial loss-of-function allele.

(B) Whole-mount in situ hybridization analysis (performed according to standard procedures with minor modifications[15]) of *Armc4* in mouse embryos (E7.5) with an *Armc4* antisense probe, made from a 547 bp pCRII construct (nt 1315–1861) by TOPO TA cloning (Invitrogen) after amplification from complementary DNA. *Armc4* is specifically expressed in the ventral node of mouse embryos (E7.5) (marked with an asterix in I) suggesting a function in left-right axis development. (I), view from the left; (II), ventral view; (III), transverse section through the node. The blue precipitate shown in I and II appears gray in III as a result of the use of a gray scale camera.
(C) Cardiac anomalies seen in *Aotea Armc4* mutant mice included mirror image dextrocardia with perimembranous (pmVSD) and multiple muscular ventricular septal defects (mVSD), ventricular noncompaction, and anomalous venous return with dual inferior vena cava (IVC). Abbreviations are as follows: A, aorta; DA, ductus arteriosus; mLA, morphological left atrium; mRA, morphological right atrium; mLV, morphological left ventricle; mRV, morphological right ventricle; LSVC, left superior vena cava; RSVC, right superior vena cava. R, right; L, left. Scale bars in (E)–(G) are 0.5 mm and in (H) and (I) are 10 μm. For EFIC (episcopic fluorescence image capture) imaging, a Leica LSI scanning confocal microscope was used to capture fluorescence images of the paraffin block face sectioned with a Leica SM2500 microtome. Images were captured serially during microtome sectioning to generate registered 2D image stacks. For 3D volume rendering, the 2D image stacks were processed with Osirix software.
(D) *Aotea Armc4* mutant exhibit severe ODA defects, typically with only a few ODAs observed (blue arrows), while WT airway typically showed 5–7 ODAs.
(E) Air-dried tracheal airway tissue from WT and *Aotea* mutant mice stained by coIF and visualized by immunofluorescence microscopy for acetylated tubulin (green) and the ODA component MDNAH5 (red). Nuclei were stained with Hoechst 33342 (blue). In control mice, MDNAH5 localizes to the axonemes stained with acetylated tubulin (top row), but in *Aotea Armc4* mutant airway epithelia, MDNAH5 is only present in the proximal part of the ciliary axonemes (bottom row).

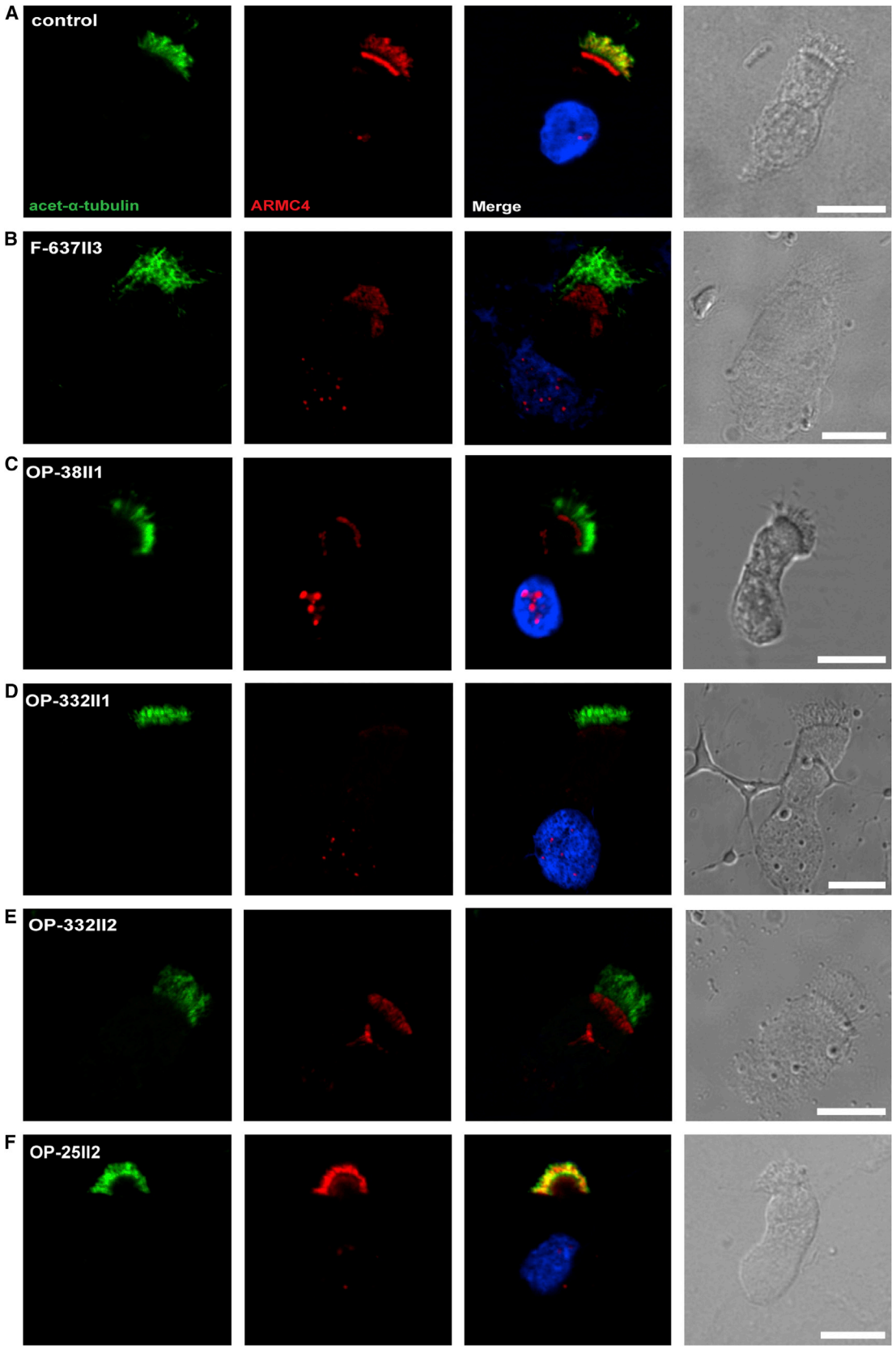

Figure 4. Subcellular Localization of ARMC4 in Respiratory Epithelial Cells from Individuals with PCD Carrying *ARMC4* Mutations
Respiratory epithelial cells from control and PCD individuals carrying *ARMC4* mutations were double-labeled with antibodies directed against acetylated tubulin (green) and ARMC4 (red) via a rabbit polyclonal antibody (Sigma HPA037829). Nuclei were stained with Hoechst 33342 (blue).

(legend continued on next page)

To elucidate further the molecular defect caused by ARMC4 deficiency, we examined the large multiprotein ODA and IDA complexes by IF microscopy by using antibodies targeting ODA (heavy chains DNAH5 and DNAH9; intermediate chain DNAI2) and IDA (light chain DNALI1) components. In all cases, we observed axonemal DNALI1 localization (Figure S4) consistent with normal IDA composition documented by TEM. In contrast, DNAH5 and DNAI2 were present proximally but absent distally from the ciliary axonemes, consistent with findings in the *Aotea Armc4* mutant mouse (Figures 5A–5D; Figures S5A–S5F and S6A and S6B). These findings indicate that *ARMC4* mutations result in partial ODA defects in respiratory cilia.

We have reported previously at least two discernible ODA types in ciliary axonemes of human respiratory cilia[27]—type 1 proximal compartments that contain DNAH5 but not DNAH9, and type 2 distal compartments that contain both DNAH5 and DNAH9. In most PCD individuals with ODA defects, both ODA types are absent from the ciliary axonemes (e.g., mutations in *DNAH5*, *DNAI2*). In other PCD individuals caused by mutations in genes encoding axonemal ODA components, such as DNAI1 or anchoring factors such as CCDC103, only type 2 ODA complexes are affected. This is also observed for ODA defects caused by defective cytoplasmic preassembly involving *DNAAF2* (*KTU*) mutations. In all of these PCD types, the ODA heavy-chain DNAH9, which normally localizes to the distal ODA type 2 complexes, is absent from the ciliary axonemes (Figure S7). Thus, it was unexpected that DNAH9 is present in the axoneme but mislocalized throughout the whole ciliary compartment in *ARMC4* mutant cilia (Figures 5E and 5F; Figures S5G, S5H, and S6C); the mislocalization of a structural ODA component (DNAH9) has not been described in other PCD types so far. This kind of ODA defect was observed in all individuals, whether with *ARMC4* truncating or missense mutations.

Given our observation that *ARMC4* mutations cause mislocalization of the ODA protein DNAH9, we posited that it is unlikely that ARMC4 represents a structural component of ODA complexes. To test this hypothesis, we examined ARMC4 localization in respiratory cells that carried well-defined dynein arm defects, caused by mutations in *DNAH5* (both types 1/2 ODA defects), *CCDC103* (type 2 ODA defect), and *DNAAF1* (type 1/2 ODA defects and IDA defects due to altered cytoplasmic preassembly) (Figure S8). The axonemal localization of ARMC4 remained unaffected in all analyzed mutant cells, indicating that ARMC4 is probably not a structural component of ODA complexes. To elucidate ARMC4 function further, we studied the axonemal localization of ARMC4 in *CCDC114* mutant cilia, and we found ARMC4 undetectable in these respiratory cilia (Figures 6A and 6B). Because CCDC114 is an ODA-microtubule docking complex component,[28,29] we suggest that ARMC4 might have a role not only in targeting but also in docking of ODA complexes. On the other hand, we studied the localization of CCDC114 in *ARMC4* mutant cilia and demonstrated that CCDC114 still localizes to the whole length of the axonemes as in the unaffected controls (Figures 6C and 6D), indicating that ODA docking complex component CCDC114 localization is not ARMC4 dependent.

On the basis of these findings, we propose that ARMC4 belongs to a class of ciliary proteins required for correct axonemal docking and targeting of ODA components and/or complexes. We have previously proposed a model for ODA assembly;[23] accordingly, ARMC4 is an example of a protein involved in a late step of axonemal ODA assembly (step III). Interestingly, ARMC4 is not found in the unicellular alga *Chlamydomonas*, a model system classically used to study ODA assembly and in which only a single ODA type is present.[2] Our findings suggest that ARMC4 has a unique function required for targeting type 2 ODAs in the human and mouse airway. The identification of mutations in *ARMC4* will aid the genetic diagnosis of PCD and provide an additional model for understanding the basic biological function of motile cilia and flagella.

Supplemental Data

Supplemental Data include eight figures, two tables, Supplemental Grant Information, and eight movies and can be found with this article online at http://www.cell.com/AJHG.

Acknowledgments

We thank the PCD-affected individuals and their families for their participation and acknowledge the German patient support group "Kartagener Syndrom und Primaere Ciliaere Dyskinesie e.V." We are grateful to investigators and the coordinators of the "Genetic Disorders of Mucociliary Clearance Consortium" that is part of the Rare Disease Clinical Research Network; its members are listed in the Supplemental Data file. We thank D. Nergenau, M. Herting, S. Weiser, F.J. Seesing, P. Fischer, W. Wolf, K. Burns, and R. Pace for excellent technical work and E. Godwin for administrative support. We would like to acknowledge Robbert de Iongh from University of Melbourne, Australia for providing DNA from PCD families, K. Landwehr from Evangelical Hospital Bielefeld, L. Greiner from Helius Klinikum Wuppertal, and H. Mitchison and A. Shoemark for providing samples of individuals with *CCDC114* mutations. This work was supported by a fellowship of the NRW Research School "Cell Dynamics and Disease, CEDAD" to R.H., by the "Deutsche Forschungsgemeinschaft" (DFG OM 6/4, OM 6/5) and the IZKF (Om2/009/12) Muenster to

(A) Both proteins colocalize (yellow) along the ciliary axonemes in cells from the unaffected controls.
(B–E) In respiratory cells of *ARMC4* individuals, ARMC4 is not detectable in the ciliary axonemes, consistent with recessive loss-of-function mutations that result in the failure to produce a functional ARMC4. However, in respiratory cells of individual OP-25II2 hypomorphic for *ARMC4* (F), ARMC4 still localizes to the ciliary axonemes. Scale bars represent 10 μm.

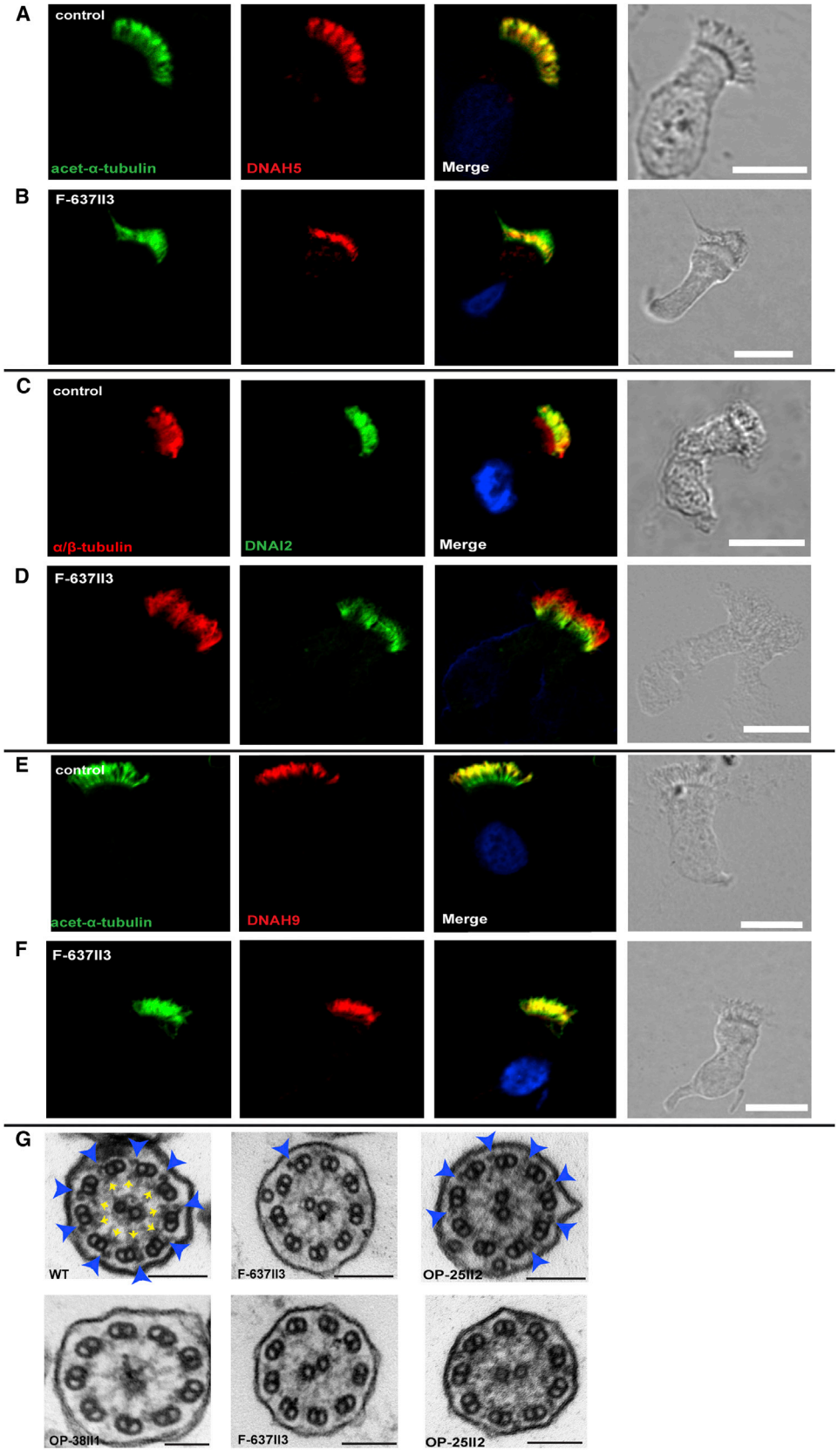

Figure 5. ***ARMC4*** **Mutations Result in Outer Dynein Arms (ODA) Defects of Respiratory Cilia**
(A–F) Localization of ODA-associated proteins (antibodies reported previously[16,27]).
(A–D) Respiratory epithelial cells from control (A and C) and PCD-affected individual F-637II3 (B and D) were double-labeled with antibodies directed against acetylated tubulin (green) and DNAH5 (red) (A and B) and α/β tubulin (red) and DNAI2 (green) (C and

(legend continued on next page)

H.O., as well as funding from EU 7th FP under GA nr. 241955, project SYSCILIA to H.O. and N.K., and under GA nr. 305404, project BESTCILIA to H.O.; the US National Institute of Health (NIH) grants U01-HL098180 (Bench to Bassinet Program) to C.W.L., 5U54HG006542 and 5R0/NS058529 to J.R.L., and DK072301 to N.K. M.R.K., M.W.L., M.R., and M.A.Z. are supported by NIH/ORDR U54 HL096458-10 and RO1 HL071798 research grants and PCD Foundation.

Received: April 3, 2013
Revised: June 3, 2013
Accepted: June 8, 2013
Published: July 11, 2013

Web Resources

The URLs for data presented herein are as follows:

1000 Genomes, http://browser.1000genomes.org
DGV (Database of Genomic Variants), http://projects.tcag.ca/variation/
Mouse Genome Informatics, http://www.informatics.jax.org//javawi2/servlet/WIFetch?page=alleleDetail&id=MGI:5311373
Online Mendelian Inheritance in Man (OMIM), http://www.omim.org/
PolyPhen-2, http://www.genetics.bwh.harvard.edu/pph2/

References

1. Pazour, G.J., Agrin, N., Leszyk, J., and Witman, G.B. (2005). Proteomic analysis of a eukaryotic cilium. J. Cell Biol. *170*, 103–113.
2. Fliegauf, M., Benzing, T., and Omran, H. (2007). When cilia go bad: cilia defects and ciliopathies. Nat. Rev. Mol. Cell Biol. *8*, 880–893.
3. Sharma, N., Berbari, N.F., and Yoder, B.K. (2008). Ciliary dysfunction in developmental abnormalities and diseases. Curr. Top. Dev. Biol. *85*, 371–427.
4. Loges, N.T., Olbrich, H., Becker-Heck, A., Haeffner, K., Heer, A., Reinhard, C., Schmidts, M., Kispert, A., Zariwala, M.A., Leigh, M.W., et al. (2009). Deletions and point mutations of LRRC50 cause primary ciliary dyskinesia due to dynein arm defects. Am. J. Hum. Genet. *85*, 883–889.
5. Noone, P.G., Leigh, M.W., Sannuti, A., Minnix, S.L., Carson, J.L., Hazucha, M., Zariwala, M.A., and Knowles, M.R. (2004). Primary ciliary dyskinesia: diagnostic and phenotypic features. Am. J. Respir. Crit. Care Med. *169*, 459–467.
6. Gherman, A., Davis, E.E., and Katsanis, N. (2006). The ciliary proteome database: an integrated community resource for the genetic and functional dissection of cilia. Nat. Genet. *38*, 961–962.
7. Ostrowski, L.E., Blackburn, K., Radde, K.M., Moyer, M.B., Schlatzer, D.M., Moseley, A., and Boucher, R.C. (2002). A proteomic analysis of human cilia: identification of novel components. Mol. Cell. Proteomics *1*, 451–465.
8. Broadhead, R., Dawe, H.R., Farr, H., Griffiths, S., Hart, S.R., Portman, N., Shaw, M.K., Ginger, M.L., Gaskell, S.J., McKean, P.G., and Gull, K. (2006). Flagellar motility is required for the viability of the bloodstream trypanosome. Nature *440*, 224–227.
9. McClintock, T.S., Glasser, C.E., Bose, S.C., and Bergman, D.A. (2008). Tissue expression patterns identify mouse cilia genes. Physiol. Genomics *32*, 198–206.
10. Lonergan, K.M., Chari, R., Deleeuw, R.J., Shadeo, A., Chi, B., Tsao, M.S., Jones, S., Marra, M., Ling, V., Ng, R., et al. (2006). Identification of novel lung genes in bronchial epithelium by serial analysis of gene expression. Am. J. Respir. Cell Mol. Biol. *35*, 651–661.
11. Tewari, R., Bailes, E., Bunting, K.A., and Coates, J.C. (2010). Armadillo-repeat protein functions: questions for little creatures. Trends Cell Biol. *20*, 470–481.
12. Yu, Q., Leatherbury, L., Tian, X., and Lo, C.W. (2008). Cardiovascular assessment of fetal mice by in utero echocardiography. Ultrasound Med. Biol. *34*, 741–752.
13. Tan, S.Y., Rosenthal, J., Zhao, X.Q., Francis, R.J., Chatterjee, B., Sabol, S.L., Linask, K.L., Bracero, L., Connelly, P.S., Daniels, M.P., et al. (2007). Heterotaxy and complex structural heart defects in a mutant mouse model of primary ciliary dyskinesia. J. Clin. Invest. *117*, 3742–3752.
14. Ibañez-Tallon, I., Pagenstecher, A., Fliegauf, M., Olbrich, H., Kispert, A., Ketelsen, U.P., North, A., Heintz, N., and Omran, H. (2004). Dysfunction of axonemal dynein heavy chain Mdnah5 inhibits ependymal flow and reveals a novel mechanism for hydrocephalus formation. Hum. Mol. Genet. *13*, 2133–2141.
15. Olbrich, H., Haeffner, K., Kispert, A., Völkel, A., Volz, A., Sazmag, G., Reinhardt, R., Hennig, S., Lehrach, H., Konietzko, N., et al. (2002). Mutations in DNAH5 cause primary ciliary dyskinesia and randomization of left-right asymmetry. Nat. Genet. *30*, 143–144.
16. Loges, N.T., Olbrich, H., Fenske, L., Mussafi, H., Horvath, J., Fliegauf, M., Kuhl, H., Baktai, G., Petterffy, E., Chodhari, R., et al. (2008). DNAI2 mutations cause primary ciliary dyskinesia with defects in the outer dynein arm. Am. J. Hum. Genet. *83*, 547–558.
17. Bartoloni, L., Blouin, J.L., Pan, Y., Gehrig, C., Maiti, A.K., Scamuffa, N., Rossier, C., Jorissen, M., Armengot, M., Meeks, M., et al. (2002). Mutations in the DNAH11 (axonemal heavy chain dynein type 11) gene cause one form of situs inversus

D). In both stainings, both proteins colocalize (yellow) along the cilia in cells from the unaffected control. In contrast, in the cells of this individual, DNAH5 and DNAI2 are not detectable in the distal part of the ciliary axonemes but still assemble in the proximal part of the ciliary axonemes.
(E and F) Sublocalization pattern of the ODA-heavy-chain protein DNAH9 in cilia of respiratory epithelial cells from control and PCD-affected individual F-637II3. Cells were double-labeled with antibodies directed against acetylated tubulin (green) and DNAH9 (red). Both proteins colocalize (yellow) on the distal part of cilia in cells from the unaffected control. Unexpectedly, in the respiratory cells of individual F-637II3 (F), DNAH9 localizes to the entire axonemal length. (A–F) Nuclei are stained with Hoechst33342 (blue).
(G) Transmission electron micrographs show defects of ODAs in three PCD individuals with *ARMC4* mutations compared to a control without PCD. In the healthy control, outer dynein arms (blue arrows) and inner dynein arms (yellow arrows) are visible. The cilia from these individuals have severe defects of the ODAs with normal composition of IDAs (lower panel). However, some of their cilia have remnants of ODAs (upper panel, blue arrows). Scale bars in (A)–(F) are 10 μm and in (G) are 0.1 μm.

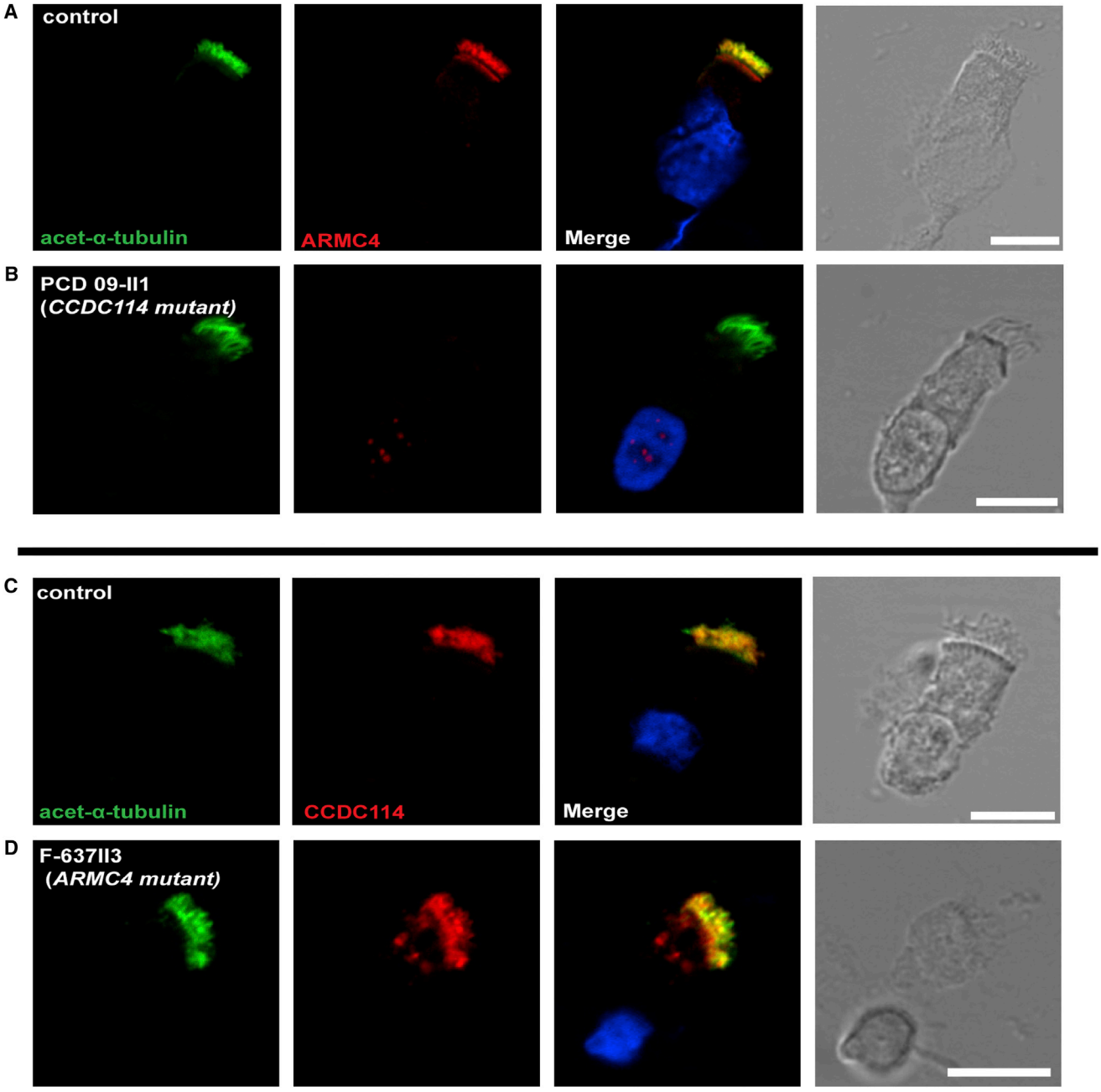

Figure 6. Mutations in *CCDC114* Encoding an ODA-Microtubule Docking Complex Component Affect ARMC4 Localization in Human Respiratory Cells.

(A and B) Respiratory epithelial cells from a control and a PCD-affected individual carrying *CCDC114* mutations (PCD 09-II1) were double-labeled with antibodies directed against acetylated tubulin (green) and ARMC4 (red).

(C and D) Respiratory epithelial cells from a control and a PCD-affected individual carrying *ARMC4* mutations (F-637II3) were double-labeled with antibodies directed against acetylated tubulin (green) and CCDC114 (red). (A,C) Both CCDC114 and ARMC4 localize (yellow) along control ciliary axonemes (B) In respiratory cells lacking CCDC114 (individual PCD 09-II1), ARMC4 is undetectable in the ciliary axonemes, indicating that ARMC4 ciliary localization is CCDC114-dependent. (D) However, in respiratory cells lacking ARMC4 (individual F-637II3), CCDC114 still localizes to the ciliary axonemes, indicating that CCDC114 ciliary localization is not ARMC4-dependent. Scale bars are 10 μm.

totalis and most likely primary ciliary dyskinesia. Proc. Natl. Acad. Sci. USA *99*, 10282–10286.

18. Pennarun, G., Escudier, E., Chapelin, C., Bridoux, A.M., Cacheux, V., Roger, G., Clement, A., Goossens, M., Amselem, S., and Duriez, B. (1999). Loss-of-function mutations in a human gene related to Chlamydomonas reinhardtii dynein IC78 result in primary ciliary dyskinesia. Am. J. Hum. Genet. *65*, 1508–1519.
19. Duriez, B., Duquesnoy, P., Escudier, E., Bridoux, A.M., Escalier, D., Rayet, I., Marcos, E., Vojtek, A.M., Bercher, J.F., and Amselem, S. (2007). A common variant in combination with a nonsense mutation in a member of the thioredoxinfamily

causes primary ciliary dyskinesia. Proc. Natl. Acad. Sci. USA *104*, 3336–3341.

20. Mazor, M., Alkrinawi, S., Chalifa-Caspi, V., Manor, E., Sheffield, V.C., Aviram, M., and Parvari, R. (2011). Primary ciliary dyskinesia caused by homozygous mutation in DNAL1, encoding dynein light chain 1. Am. J. Hum. Genet. *88*, 599–607.
21. Panizzi, J.R., Becker-Heck, A., Castleman, V.H., Al-Mutairi, D.A., Liu, Y., Loges, N.T., Pathak, N., Austin-Tse, C., Sheridan, E., Schmidts, M., et al. (2012). CCDC103 mutations cause primary ciliary dyskinesia by disrupting assembly of ciliary dynein arms. Nat. Genet. *44*, 714–719.
22. Knowles, M.R., Leigh, M.V., Ostrowski, L.E., Huang, L., Carson, J.L., Hazucha, M.J., Yin, W., Berg, J.S., Davis, S.D., Dell, S.D., et al. (2013). Exome sequencing identifies mutations in *CCDC114* as a cause of primary ciliary dyskinesia. Am. J. Hum. Genet. *92*, 99–106.
23. Omran, H., Kobayashi, D., Olbrich, H., Tsukahara, T., Loges, N.T., Hagiwara, H., Zhang, Q., Leblond, G., O'Toole, E., Hara, C., et al. (2008). Ktu/PF13 is required for cytoplasmic pre-assembly of axonemal dyneins. Nature *456*, 611–616.
24. Mitchison, H.M., Schmidts, M., Loges, N.T., Freshour, J., Dritsoula, A., Hirst, R.A., O'Callaghan, C., Blau, H., Al Dabbagh, M., Olbrich, H., et al. (2012). Mutations in axonemal dynein assembly factor DNAAF3 cause primary ciliary dyskinesia. Nat. Genet. *44*, 381–389.
25. Horani, A., Druley, T.E., Zariwala, M.A., Patel, A.C., Levinson, B.T., Van Arendonk, L.G., Thornton, K.C., Giacalone, J.C., Albee, A.J., Wilson, K.S., et al. (2012). Whole-exome capture and sequencing identifies *HEATR2* mutation as a cause of primary ciliary dyskinesia. Am. J. Hum. Genet. *91*, 685–693.
26. Kott, E., Duquesnoy, P., Copin, B., Legendre, M., Dastot-Le Moal, F., Montantin, G., Jeanson, L., Tamalet, A., Papon, J.F., Siffroi, J.P., et al. (2012). Loss-of-function mutations in LRRC6, a gene essential for proper axonemal assembly of inner and outer dynein arms, cause primary ciliary dyskinesia. Am. J. Hum. Genet. *91*, 958–964.
27. Fliegauf, M., Olbrich, H., Horvath, J., Wildhaber, J.H., Zariwala, M.A., Kennedy, M., Knowles, M.R., and Omran, H. (2005). Mislocalization of DNAH5 and DNAH9 in respiratory cells from patients with primary ciliary dyskinesia. Am. J. Respir. Crit. Care Med. *171*, 1343–1349.
28. Onoufriadis, A., Paff, T., Antony, D., Shoemark, A., Micha, D., Kuyt, B., Schmidts, M., Petridi, S., Dankert-Roelse, J.E., Haarman, E.G., et al. (2013). Splice-site mutations in the axonemal outer dynein arm docking complex gene CCDC114 cause primary ciliary dyskinesia. Am. J. Hum. Genet. *92*, 88–98.
29. Knowles, M.R., Leigh, M.W., Ostrowski, L.E., Huang, L., Carson, J.L., Hazucha, M.J., Yin, W., Berg, J.S., Davis, S.D., Dell, S.D., et al. (2013). Exome sequencing identifies mutations in CCDC114 as a cause of primary ciliary dyskinesia. Am. J. Hum. Genet. *92*, 99–106.